The Effect of Thermal History on the Distribution of Residual Stresses in PMMA Rods

RAMESH K. MITTAL* and VIBHU RASHMI,† *Indian Institute of Technology, Hauz Khas, New Delhi-110016, India*

Synopsis

A nondestructive technique based on the photoelastic properties of transparent polymers has been used to monitor the distribution of residual stress components in circular rods of poly(methyl methacrylate) (PMMA). The influence of various thermal histories on these stresses as well as on the molecular birefringence has been determined. The technique has been further simplified to obtain the values of maximum tensile and compressive residual stresses with the help of just two photoelastic measurements. The stresses so obtained are within 10% of the values obtained using detailed experimental measurements and their analysis. The simplified procedure is, therefore, suitable for "on-line" determination of residual stresses in extrusion industry.

INTRODUCTION

In a recent study[1] a photoelastic technique has been established to determine experimentally the distribution of residual stresses in circular rods of transparent polymers like poly(methyl methacrylate) (PMMA). This technique is nondestructive as compared to the commonly used layer removal technique. The layer removal technique is also very time-consuming since it involves careful machining by which the mechanical equilibrium of the specimen is disturbed and it takes a long time for the equilibrium to be established again due to the viscoelastic nature of polymers. Furthermore, it is necessary to measure very small deformations after a layer is removed and hence high accuracy is not always possible.

On the other hand, the photoelastic method is easy to apply, quite accurate, and does not require any additional operations. But it has the limitation that it can be applied only to rods and tubes of transparent polymers exhibiting photoelastic effect, e.g., poly(methyl methacrylate), polystyrene, polycarbonate, etc. The present study deals with the application of the photoelastic technique to ascertain the effect of thermal history on the residual stresses in poly(methyl methacrylate) (PMMA) rods. Since the same specimen can be used for various thermal treatments, the effect of other material parameters is kept to the minimum. Also, it is possible to obtain not only the distribution of the axial component of residual stress but also the radial and hoop stress distributions. As a byproduct of the technique information is also obtained about the degree of molecular birefringence in the specimen.

*Department of Applied Mechanics.
†Industrial Tribology, Machine Dynamics and Maintenance Engineering Centre.

Journal of Applied Polymer Science, Vol. 34, 627–638 (1987)

CCC 0021-8995/87/020627-12$04.00

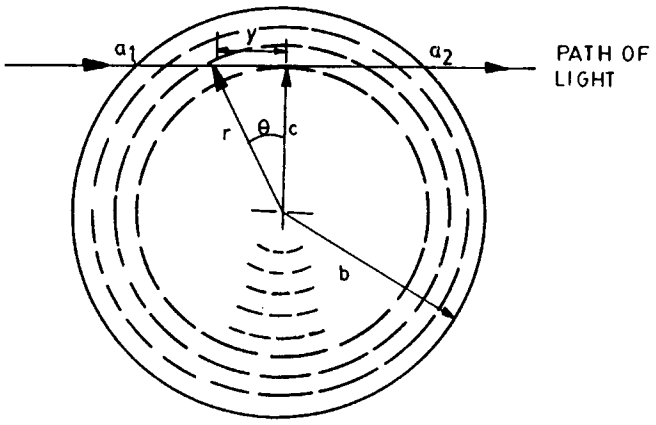

Fig. 1. A typical path of light through cylindrical rod, showing notations used and the arrangement of rings.

On the basis of measurements reported in this paper, a formula is also given to quickly determine the maximum compressive or tensile residual stresses in a rod, thus enhancing the value of the photoelastic method as a quality control method for the industry engaged in the extrusion of transparent polymers.

PHOTOELASTIC TECHNIQUE AND ITS BASIC ANALYSIS

The photoelastic technique essentially consists of measuring the total birefringence at various points on a diameter of the specimen, which is in the form of circular rod or tube. This measurement can be conveniently carried out on a standard polariscope.[2] The specimen is immersed in a glass tank containing a fluid of the same refractive index as that of the specimen in order to eliminate refraction effects at curved surfaces of the specimen. However, this technique cannot be applied in regions very near the ends of the rod or tube due to certain restrictions on the analysis. This point will be elaborated further in a later section.

The basic analysis to obtain the distribution of stresses from the distribution of total birefringence R suffered by a ray of light in passing through a stressed rod of photoelastic material was developed by O'Rourke and Saenz[3] as well as Sutton.[4] For a long cylindrical rod of a circular cross section and a uniform thermal history along its length, the state of stress is completely described by σ_r, σ_θ, and σ_z components where r, θ, and z are the usual polar coordinates. In Figure 1 is shown a typical cross section of the rod. A ray of light a_1a_2 at a normal distance c from the center experiences birefringence which, according to the Maxwell–Neumann law,[2] is proportional to the difference in secondary principal stresses, i.e., $\sigma_z - (\sigma_r \cos^2\theta + \sigma_\theta \sin^2\theta)$. Since the stresses and θ are varying along the path, the total birefringence $R(c)$ along a_1a_2 is

$$R(c) = \beta \int_{a_1}^{a_2} \sigma_z - \left(\sigma_r \cos^2\theta + \sigma_\theta \sin^2\theta\right) dy \tag{1}$$

where β is the proportionality constant called the stress-optic coefficient of the rod material. In this analysis β is assumed to be uniform.

It is shown in the Appendix that the influence of σ_r and σ_θ averages out along any straight path to yield the following simple result:

$$R(c) = \beta \int_{a_1}^{a_2} \sigma_z \, dy \tag{2}$$

Mittal and Rashmi[1] have used a numerical method to obtain the residual stress component σ_z from the experimentally determined function $R(c)$. This procedure overcomes the difficulties of the one suggested by Sutton,[4] and it essentially consists of dividing the circular cross section into n concentric rings (Fig. 1). If σ_i is the average value of σ_z in the ith ring and Δy_i is length of the light path through the same ring, then eq. (2) can be rewritten as

$$R(c) = \beta \sum_{i=1}^{n} \sigma_i \Delta y_i \tag{3}$$

The values of σ_i are obtained from eq. (3) by a simple computer program. However, before applying the program, the value of σ_1, i.e., the axial stress in the outermost ring or the surface stress must be estimated *a priori*, and the accuracy of the numerical method depends on the accuracy of this estimate. It is shown in Ref. 1 that this value is obtained accurately by first plotting the average birefringence per unit length, i.e., $R(c)/2\sqrt{b^2 - c^2}$ as a function of the distance of the light path from the center of the specimen and then extrapolating the curve to the surface of the specimen. This limiting value of the average birefringence is proportional to the value of σ_z at the surface.

Further, Sutton[4] has shown that the net area under the $R(c)$ vs. c curve should be zero for a solid rod if the "sum rule" of stresses, i.e.,

$$\sigma_z = \sigma_r + \sigma_\theta \tag{4}$$

is applicable. While O'Rourk and Saenz[3] assumed the validity of this rule, Sutton[4] established that the rule is valid for a long cylinder if the stresses are due to thermoelastic phenomena only. Recently Williams[5] has analyzed theoretically the development of residual stresses taking into account the viscoelastic effects. His results explicitly show that for a long circular rod or tube the sum rule is satisfied. Thus, there is a justification to attribute a nonzero net area under $R(c)$ curve to the presence of birefringence caused by phenomena other than the thermoviscoelastic stress formation. One such possibility is the molecular orientations which get frozen in as the polymer sets. Isayev and Crouthamel[6] refer to this phenomenon as one caused by "flow-induced stresses."

Another consequence of the sum rule is that once the σ_z distribution is known it is possible to get σ_r and σ_θ distributions also. The following equation is obtained easily from the equation of equilibrium and eq. (4):

$$\sigma_r(\rho) = \frac{1}{\rho^2} \int_b^\rho r\sigma_z(r) \, dr \tag{5}$$

On the basis of these observations, the following procedure of analysis was

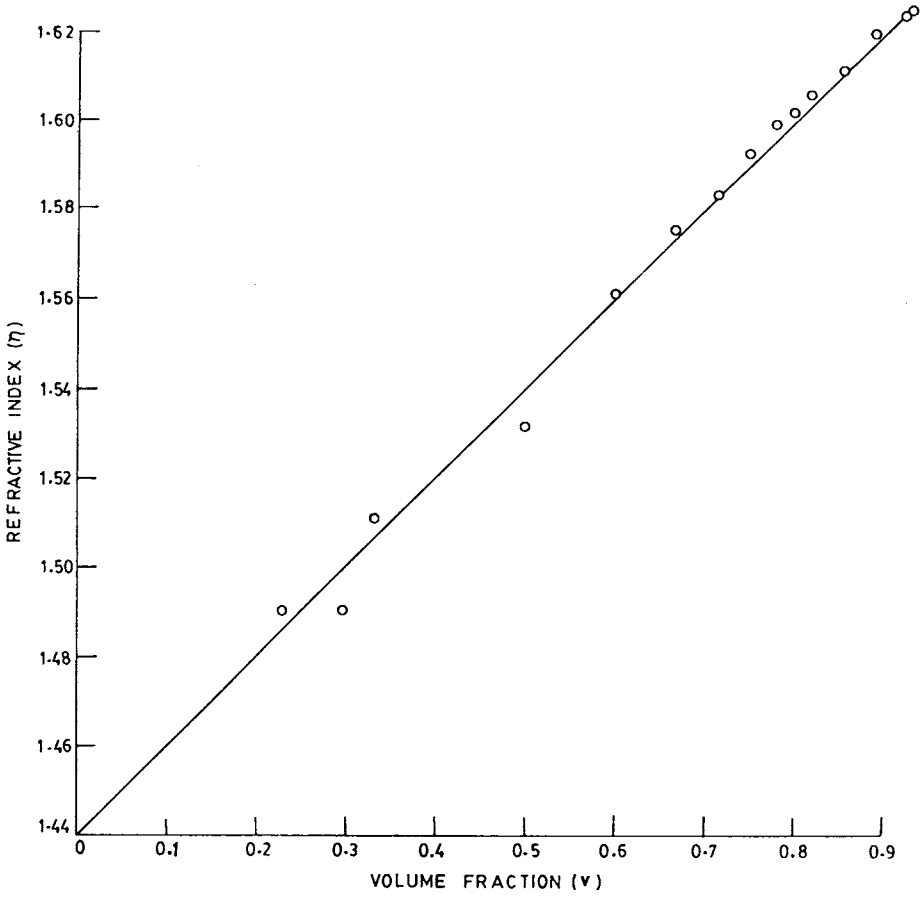

Fig. 2. Variation of the refractive index of the mixture of α-bromnapthalene and liquid paraffin with the volume fraction of α-bromnapthalene.

adopted in the present work:

(i) From $R(c)$, curve σ_z was obtained numerically.
(ii) The net area under the $R(c)$ curve was determined. This area represents the molecular orientation in the specimen.
(iii) From σ_z curve the radial stress distribution, σ_r was obtained.
(iv) σ_θ distribution was obtained using $\sigma_\theta = \sigma_z - \sigma_r$.

EXPERIMENTAL RESULTS

The experiments were carried out on five commercially available solid rods of PMMA. The rods were checked to be free from crazes and other extrusion defects. For each rod a matching fluid was prepared from mixture of α-bromnapthalene and liquid paraffin. This work was facilitated by using the linear curve of Figure 2, where the refractive index (η) of the mixture is plotted as a function the volume fraction (v) of α-bromnapthalene. When the fluid of matching refractive index has been properly selected, the PMMA rod becomes indistinguishable from the fluid when submerged in it. During the

course of this series of experiments, it was also observed that the accuracy of birefringence measurements is very much dependent on the closeness of index matching. Further, the fluids or their mixture should not chemically react or diffuse through the submerged surface of the rod at least for the duration of the experiment ($\sim 1/4$ h). With the diffusion of the fluid plasticization can take place followed by the relaxation of stresses. To check this possibility in the present work, a quenched rod of PMMA was first allowed to relax for 2 days in air so that further relaxation was negligible. Then it was submerged in the selected matching fluid. The birefringence distribution was regularly monitored for more than 24 h. No discernible change was observed in $R(c)$ curves, showing that the mixture was quite safe.

In order to complete the analysis, it is necessary to measure the stress optic coefficient β of each rod. This was achieved by the diameteral compression of a disc cut from the rod and measuring the fringe order variation at the center of the disc with the applied load. The relevant analysis is given in Ref. 2.

For reference, the five rods have been designated as P1, P2, P3, P4, and P5 and the states for which the birefringence measurements were taken as A, B, C, D, and E. State A is the "as extruded" state while for other states the specimen was slowly heated to 120°C and maintained at this temperature for 2 h. However rod P5 was kept at 120°C for 4 h since its diameter is much larger than that of others. After heating the rods are either quenched or cooled gradually. For state B the quenching bath was maintained at 2°C while for C quenching was to room temperature. States D and E correspond, respectively, to air cooling and cooling inside the oven at a uniform rate of 8°C/h. State E is also referred to as the annealed state.

Figure 3 shows a series of birefringence and average birefringence curves for a typical rod (P2). The effect of heat treatments on these curves is very obvious. Similar effects were observed for other rods too. The experimental values of $R(c)$ were analyzed numerically to obtain σ_z, σ_r, and σ_θ curves. Figure 4 shows the variation of axial stress σ_z and radial stress σ_r for all states considered. It was estimated that a complete analysis of each state takes less than 0.5 h after a little experience. A similar exercise with layer removal technique takes several days if the specimen is allowed to relax to a stable state of stress before the next layer is removed. The results obtained by the photoelastic method are also very reproducible.

In Table I the summary of results is given for all specimens and states of heat treatment considered in this study. The net area under the birefringence curve is also included in the table. It is easily seen that the thermal history has a significant influence not only on the maximum tensile and compressive stresses but also on the net birefringence caused by the molecular state of the material.

APPLICATION TO QUALITY CONTROL

The photoelastic technique discussed in this paper can be simplified further to serve as a tool for quickly determining the effect of heat treatment or other process parameters during extrusion of rods and tubes of transparent polymers or inorganic glasses. With the help of this simplified procedure the maximum tensile and compressive stresses in a specimen are determined from

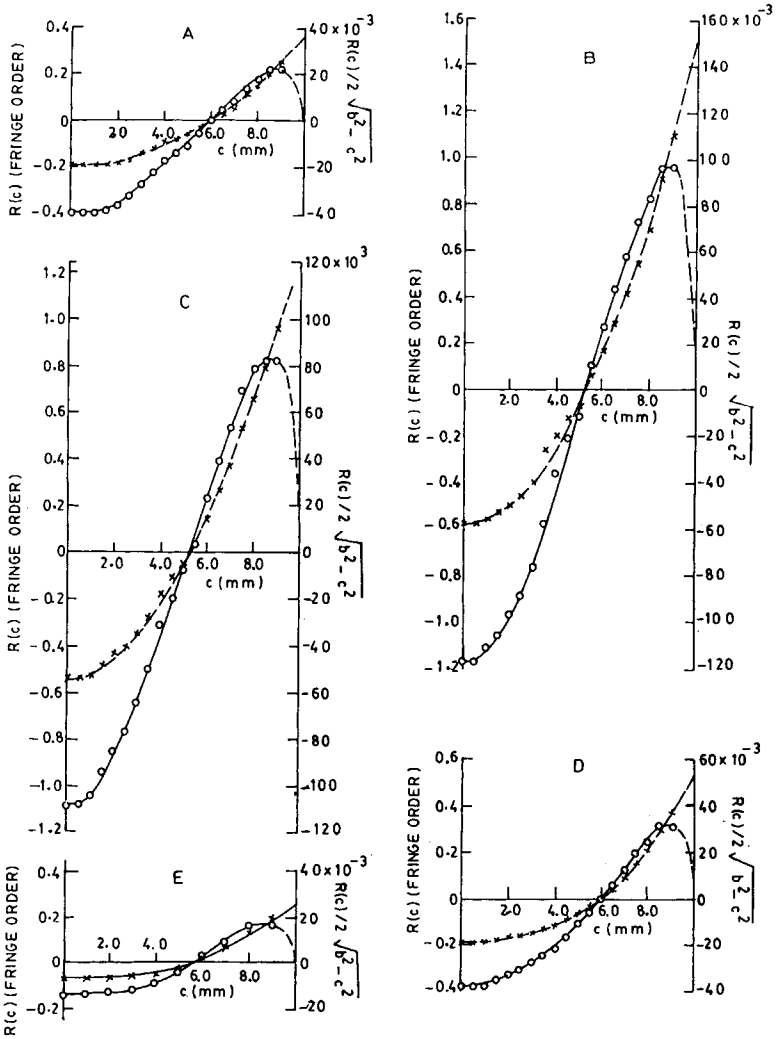

Fig. 3. Effect of various heat treatments on the distribution of total birefringence (○) and the average birefringence per unit path length (×) for rod P2. Notations A, B, C, D, and E are explained in the text.

just two experimental values of birefringence instead of the entire $R(c)$ curve. The computer program is also dispensed with. The following semiempirical formula is used:

$$(\sigma_{z_{\max}})_{T,C} = \frac{3f}{2b}(R_{\max})_{T,C} \tag{6}$$

where f is the material fringe value and b the radius of the rod. Subscripts T and C correspond respectively to tension and compression. In eq. (6) the maximum value of tensile birefringence (in fringe orders) occuring at the center of the rod is used for calculating the maximum tensile residual stress while for maximum compressive residual stress the maximum compressive

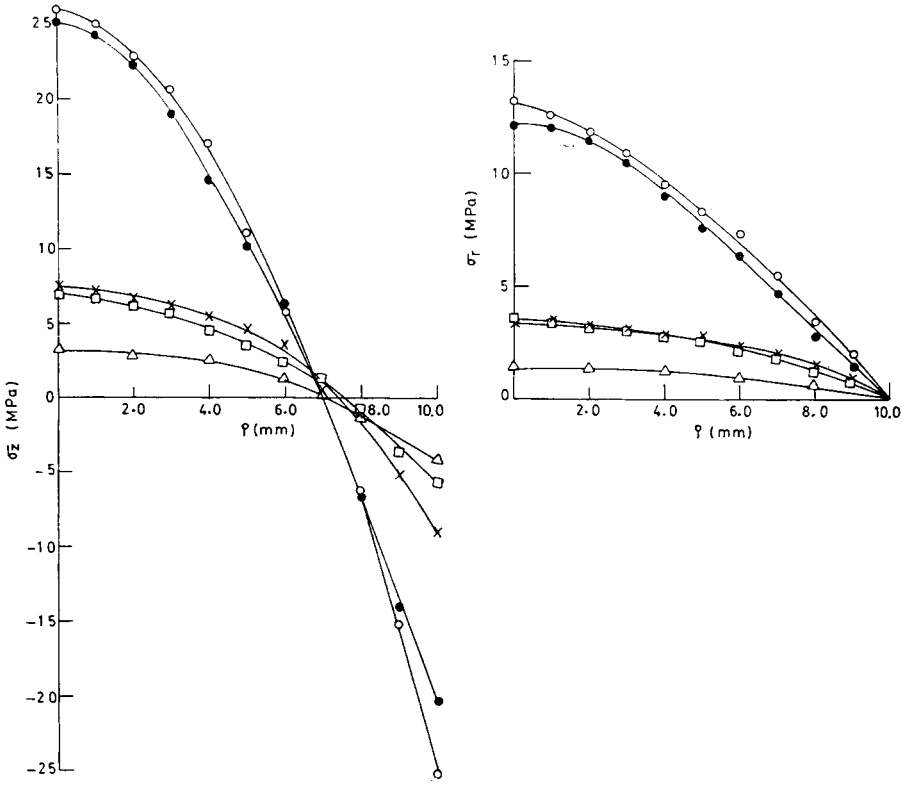

Fig. 4. Distributions of axial stress (σ_z) and radial stress (σ_r) in rod P2 when it is subjected to various heat treatments (see text): (□) A; (○) B; (●) C; (×) D; (△) E.

birefringence is used. This always lies at some distance from the surface of the rod as can be confirmed from Figure 3. The maximum compressive birefringence can be measured conveniently during fringe order compensation by either the Tardy or Senarmont[2] methods. Two parallel fringes near the surface of the rod are observed during compensation, and the analyzer rotation causing both these fringes to overlap corresponds to $(R_{\max})_C$.

Formula (6) is semiempirical, because for materials like inorganic glasses for which the effect of molecular birefringence is negligible and the distribution of residual stresses is very close to parabolic, this formula is exact. For a parabolic distribution of residual stresses $(R_{\max})_T = (R_{\max})_C$ and the zero order fringe is always located at $0.5b$, as shown in Ref. 1. In such a case it is sufficient to measure only the birefringence at the center of the rod to obtain maximum values of all stresses.

When eq. (6) is applied to the measured values of $(R_{\max})_T$ and $(R_{\max})_C$, as given in Table I, it is found that the actual values of $(\sigma_{z_{\max}})_T$ and $(\sigma_{z_{\max}})_C$ obtained from a detailed analysis lie within about 10% of the values resulting from the simplified analysis. This is shown in Figure 5, where the maximum birefringence per unit rod diameter, i.e., $R_{\max}/2b$ for all rods is plotted against the stresses calculated by the detailed analysis.

TABLE I
Summary of Maximum Birefringence and Stress Values for Various Rods

Sample no.	Rod designation[a]	Rod diameter (mm)	Maximum fringe order		Net area under birefringence curve f.o. mm	Maximum stress (MPa)	
			Compressive	Tensile		Compressive	Tensile
1	P1A	19.0	0.82	−1.0	−0.59	20.8	22.8
	P1B		0.96	−1.06	−0.19	25.5	29.9
	P1C		0.75	−0.94	−0.5	20.3	24.0
	P1D		0.38	−0.39	−0.48	10.4	9.4
	P1E		0.15	−0.13	−0.15	4.2	2.7
2	P2A	20.0	0.22	−0.39	−0.93	6.1	7.2
	P2B		0.96	−1.17	−1.09	25.3	27.3
	P2C		0.83	−1.08	−0.92	20.9	25.1
	P2D		0.32	−0.38	−0.7	9.0	7.4
	P2E		0.17	−0.14	−0.16	4.3	3.3
3	P3A	25.5	0.47	−0.61	−1.04	9.0	12.4
	P3B		1.17	−1.21	−0.81	25.9	23.3
	P3C		0.89	−1.0	−0.66	19.2	18.7
	P3D		0.68	−0.83	−0.75	13.5	18.0
	P3E		0.19	−0.19	−0.20	4.4	4.2
4	P4A	30.0	1.0	−0.44	+4.06	21.0	11.2
	P4B		1.22	−1.44	−2.39	26.5	25.3
	P4C		1.02	−1.1	−0.43	22.3	19.9
	P4D		0.69	−0.65	−0.29	14.3	10.0
	P4E		0.23	−0.45	−0.36	5.3	2.6
5	P5A	50.0	1.06	−1.67	−9.32	11.9	12.6
	P5B		1.92	−1.56	+3.08	22.0	20.4
	P5C		1.59	−1.47	−2.1	19.1	17.6
	P5D		1.14	−1.37	−4.24	13.3	14.6
	P5E		0.03	−0.45	−4.514	0.46	4.0

[a]A = extruded; B = after quenching in water at 2°C; C = after quenching in water at room temperature; D = after quenching in air at room temperature; E = after annealing in oven at room temperature.

ABOUT END EFFECTS

Finally, some observations about the end effects are noteworthy. Near the ends of the rod the fringes are curved and irregular in shape as can be observed in Figure 6(a). Away from the ends they are straight and parallel [Fig. 6(b)], indicating that the plane strain conditions are applicable and hence the analysis, either exact or simplified, can be used. There are two reasons for the stress distribution in the end region to be different from that away from the ends. First, during any heat-treatment the heat transfer phenomenon at the ends is different from that in the central region. Second, although net force and net moment due to residual stresses across any cross section including the rod ends vanish, there is an additional condition to be satisfied on the end surfaces, i.e., all points are stress-free. From Figure 6 it is seen that in the end regions extending over nearly two diameters on each side of the rod the stresses develop from a stress-free state to the stressed state, which is uniform over the rest of the rod. This region of development is also

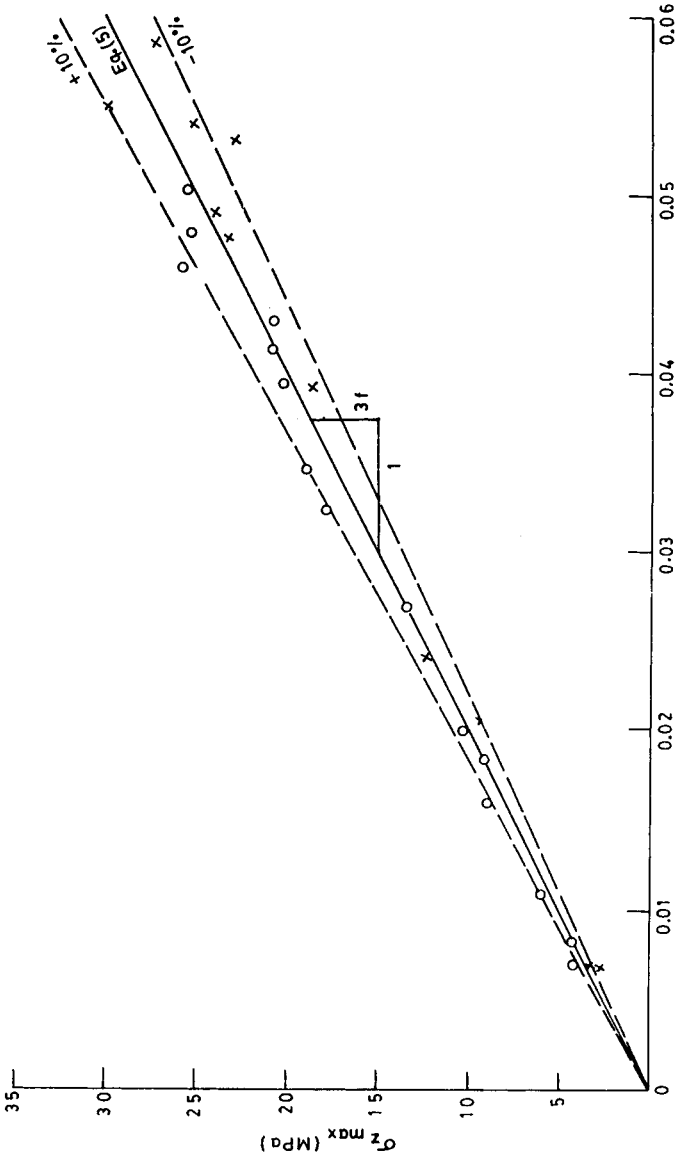

Fig. 5. Comparison of the stresses determined from eq. (5) with those obtained from a detailed analysis: (×) tension; (○) compression.

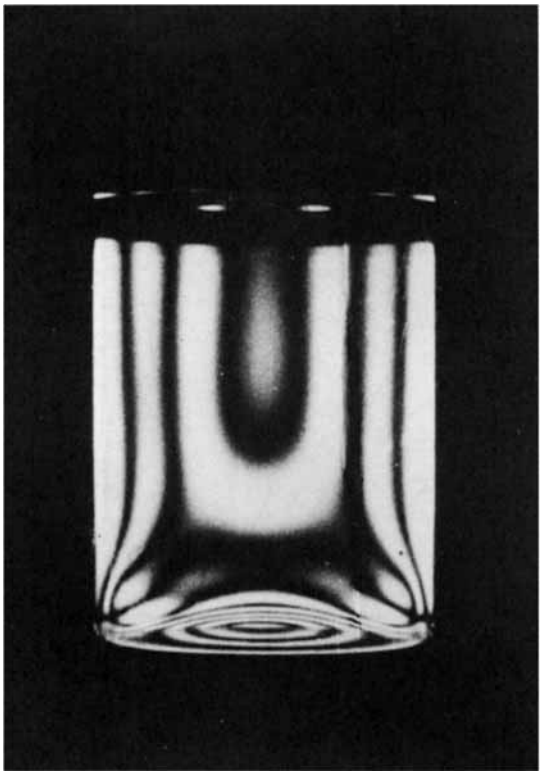

(a)

Fig. 6. Dark-field isochromatic fringe patterns: (a) near the end of the rod; (b) away from the end.

observed for applied mechanical or thermal loads and is a manifestation of St. Venant's principle.[7]

CONCLUSIONS

Two principal objectives of this study, viz., to evaluate the effect of heat treatment on the state of residual stresses and to evolve a simple experimental technique for quickly determining the maximum stresses have been fulfilled. Along with the measurement of residual stresses, the degree of molecular alignment has also been quantified. The simplified photoelastic procedure requires the measurement of birefringence values at the center of the rod and near the surface of the rod where two parallel fringes overlap. These measurements are sufficient to give the maximum stresses which are often the most significant parameters. Many properties of polymers depend on the maximum tensile or compressive stresses.[8-10] The photoelastic technique, in spite of its limitation of being applicable to transparent polymers only, is very useful due to its nondestructive nature. Certain phenomena like relaxation of quenching stresses can be investigated better with the help of this technique as compared to other techniques like layer removal in which the equilibrium of stresses has to be disturbed again and again. This aspect is under investigation, and the results will be reported in a separate publication.

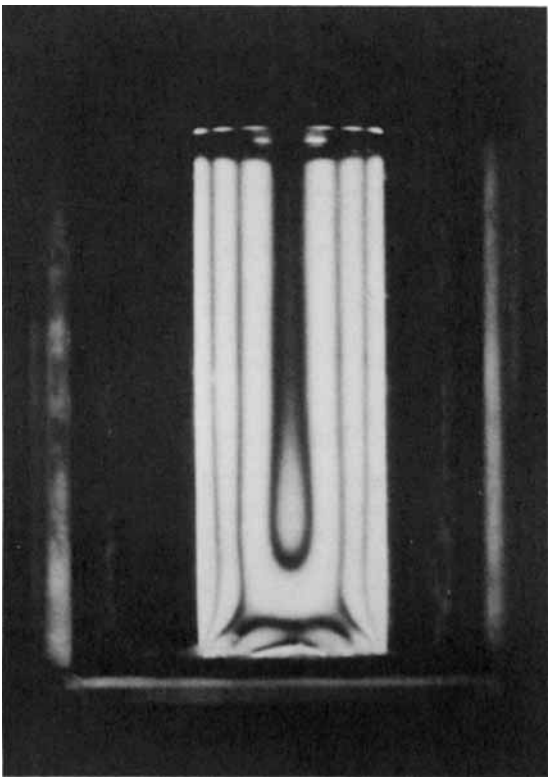

(b)

Fig. 6. (*Continued from the previous page.*)

APPENDIX

Considering the last two terms in eq. (1) and rewriting them as I, we have

$$I = \beta \int_{a_1}^{a_2} \left(\sigma_r \cos^2 \theta + \sigma_\theta \sin^2 \theta \right) dy$$

$$= 2\beta \int_0^{\sqrt{b^2 - c^2}} \left(\sigma_r \cos^2 \theta + \sigma_\theta \sin^2 \theta \right) dy \tag{7}$$

where $\sqrt{b^2 - c^2}$ is the half-length of light path (Fig. 1). From the equation of equilibrium in cylindrical polar coordinates,[7]

$$\frac{d\sigma_r}{dr} + \frac{\sigma_r - \sigma_\theta}{r} = 0$$

or

$$\frac{d(r\sigma_r)}{dr} = \sigma_\theta \tag{8}$$

Also from Figure 1, $y^2 = r^2 - c^2$ and hence $dy = (r/y)\, dr$. Changing the

variable of integration from y to r in eq. (7) and using eq. (8), we get

$$I = 2\beta \int_c^b \left[\sigma_r \frac{c^2}{ry} + \frac{y}{r} \cdot \frac{d}{dr}(r\sigma_r) \right] dr \tag{9}$$

Integration by parts and some simplification yields

$$I = 2\beta\sigma_r(b)$$

where $\sigma_r(b)$ is the radial stress at the outer surface which vanishes in the absence of any applied load on the surface of the rod. Hence, $I = 0$, and eq. (2) is established.

References

1. R. K. Mittal and V. Rashmi, *Polym. Eng. Sci.*, **26**, 310 (1986).
2. J. W. Dally and W. F. Riley, *Experimental Stress Analysis*, McGraw-Hill, New York, 1978.
3. R. C. O'Rourke and A. W. Saenz, *Quart. Appl. Math.*, **8**, 303 (1950).
4. P. M. Sutton, *J. Am. Ceram. Soc.*, **41**, 103 (1958).
5. J. G. Williams, *Plast. Rubber Process. Appl.*, **1**, 369 (1981).
6. A. I. Isayev and D. L. Crouthamel, *Polym. Plast. Technol. Eng.*, **22**, 177 (1984).
7. S. Timoshenko and J. N. Goodier, *Theory of Elasticity*, McGraw-Hill, New York, 1951.
8. P. So and L. J. Broutman, *Polym. Eng. Sci.*, **16**, 785 (1976).
9. B. S. Thakkar and L. J. Broutman, *Polym. Eng. Sci.*, **20**, 1214 (1980).
10. A. Siegman, A. Buchman, and S. Kenig, *Polym. Eng. Sci.*, **21**, 997 (1981).

Received August 11, 1986
Accepted November 24, 1986